World Academy of Science, Engineering and Technology
International Journal of Civil and Environmental Engineering
Vol:4, No:8, 2010

Error Propagation of the Hidden-Point Bar Method: Effect of Bar Geometry

Said M. Easa and Ahmed Shaker

***Abstract*—**The hidden-point bar method is useful in many surveying applications. The method involves determining the coordinates of a hidden point as a function of horizontal and vertical angles measured to three fixed points on the bar. Using these measurements, the procedure involves calculating the slant angles, the distances from the station to the fixed points, the coordinates of the fixed points, and then the coordinates of the hidden point. The propagation of the measurement errors in this complex process has not been fully investigated in the literature. This paper evaluates the effect of the bar geometry on the position accuracy of the hidden point which depends on the measurement errors of the horizontal and vertical angles. The results are used to establish some guidelines regarding the inclination angle of the bar and the location of the observed points that provide the best accuracy.

***Keywords*—**Hidden point, accuracy, error propagation, surveying, evaluation, simulation, geometry.

I. INTRODUCTION

DETERMINATION of the precise three-dimensional (3D) coordinates of a hidden point is a challenge task in land surveying. Basically, two methods have been used to determine the coordinates of a hidden point: mirror observations and hidden-point bar. The advantage of the hidden-point bar method is that the target point may not be visible from the measurement instrument [1]. Furthermore, the bar may not be settled vertically on the point target.

Generally, the hidden-point bar method can be performed using three different techniques: (a) by observing marked points on the bar at known positions using two theodolites, (b) by fitting a sphere, with a radius equal to the length of the bar and the center is at the hidden point, to a set of pre-defined points on the bar, or (c) by observing a number of points on the bar using only one theodolite. The later technique is the most cost-effective and reliable one because it needs only one theodolite instrument and it is applicable for most practical cases, especially when the free space to setup both the theodolite and the bar is limited.

S. M. Easa is Professor with the Civil Engineering Department, Ryerson University, Toronto, Canada (phone: 416-979-5000; fax: 416-979-5122; e-mail: seasa@ryerson.ca).

A Shaker is Assistant Professor with the Civil Engineering Department, Ryerson University, Toronto, Canada (e-mail: ahmed.shaker@ryerson.ca).

The research related to the hidden-point bar method has been limited. Teskey et al. [2] has investigated the precise heighting using the hidden point bar method. The investigation included development of the mathematical model, calibration of the hidden point bar using double resection [3], and comparison with precise leveling and precise trigonometric heighting. The method was applied in the field and the authors concluded that the hidden point bar method for precise heighting could be applied in industrial surveys where the required level of precision is on the order of 0.1 mm.

Teskey et al. [4] has further investigated the 3D positioning by the hidden point bar method. The investigation included development of both closed form and least-squares solutions, and calibration of the hidden point bar. The method was applied in the field at the University of Calgary Central Heating and Cooling Plant. Known movements were introduced and then recovered using the hidden-point bar method. The differences between the known and recovered movements were found to be 0.11 mm or less.

Antonopoulos [5] has applied the least squares adjustment with constraints to determine the coordinates of inaccessible points. The author used conventional methods of coordinate determination to check the efficiency of the method. The results showed that in this adjustment (normally of low redundancy) the assignment of accurate provisional values to the hidden-point coordinates constituted an essential task.

Recently, Recoskie et al. [6] performed laboratory and field measurements to test a three-prism reflector probe. This configuration allowed redundancy in the observations that required the use of the least-squares adjustment. The results indicated the need for improving the construction of the probe to ensure collinearity of the prisms

This paper focuses on the effect of the measurement errors of the observed horizontal and vertical angles on the overall accuracy of the determined coordinates of the hidden point using error propagation. Specifically, the paper investigates the effect of changing the locations of the fixed points on the bar and the effect of the bar inclination on the overall accuracy of the hidden point. A simulation approach was developed, along with a MATLAB program, to generate different observations and to estimate the corresponding errors in the determined hidden point. The following sections describe the details of the developed evaluation method, followed by the analysis results and the conclusions.

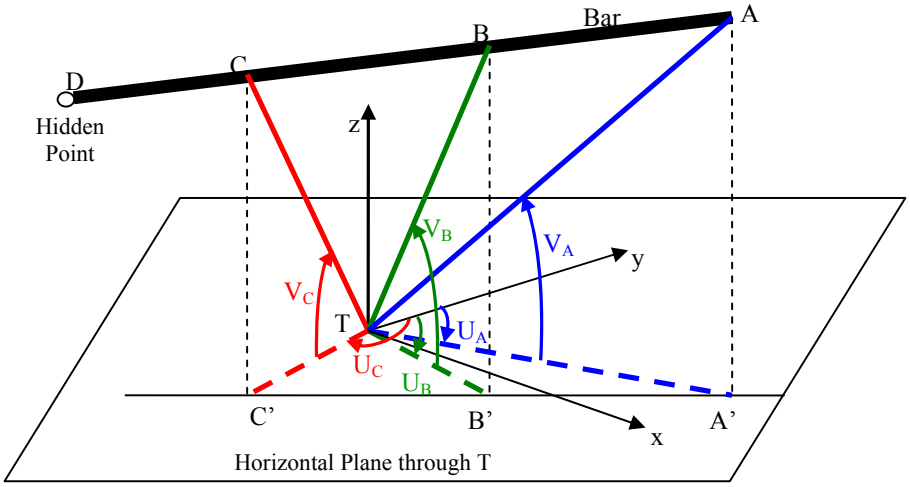

Fig. 1 Geometry of the hidden-point bar method

II. HIDDEN-POINT BAR METHOD

The geometry of the hidden-point bar method is shown in Fig. 1. It is required to determine the coordinates of the hidden point D. The bar is placed on D at a convenient orientation. Consider a 3D Cartesian right-handed *xyz* coordinate system whose origin is located at *T*, where the *z* axis is directed upwards and the *y* axis is defined by its bearing U_o to a given direction (for convenience, $U_o = 0$).

The horizontal and vertical angles are measured to three points *A*, *B*, and *C* on the bar from one station (e.g. theodolite) setup at *T*. The horizontal angles (U_A, U_B, and U_C) are measured from the *y*-axis and the vertical angles (V_A, V_B, and V_C) are measured from the horizontal plane. The distances between A and B (S_{AB}) and between B and C (S_{BC}) are known, and so is the distance between C and D (S_{CD}). The solution method is as follows [5]. The slant angles *ATB* and *BTC* are computed based on spherical trigonometry by

$$ATB = \cos^{-1}[\sin(V_A)\sin(V_B) + \cos(V_A)\cos(V_B)\cos(U_B - U_A)] \quad (1)$$

$$BTC = \cos^{-1}[\sin(V_B)\sin(V_C) + \cos(V_B)\cos(V_C)\cos(U_C - U_B)] \quad (2)$$

The angles *TCA*, *CAT*, and *TBA* are then determined by resection, based on the fact that *A*, *B*, and *C* lie on a straight line, as follows [1]

$$TCA = \cot^{-1}\{K + \cos(R)\} / \sin(R)\} \quad (3)$$

where

$$K = [S_{BC}\sin(ATB)] / [S_{AB}\sin(BTC)] \quad (4)$$

$$R = 180° - (ATB + BTC) \quad (5)$$

Then,

$$TAC = TAB = R - TCA \quad (6)$$

$$TBA = 180° - (TAB + ATB) \quad (7)$$

Subsequently, the lengths S_{TA}, S_{TB}, and S_{TC} are computed using the sin law as

$$S_{TA} = S_{AB}\sin(TBA) / \sin(ATB) \quad (8)$$

$$S_{TB} = S_{AB}\sin(TAB) / \sin(ATB) \quad (9)$$

$$S_{TC} = S_{BC}\sin(180° - TBA) / \sin(BTC) \quad (10)$$

The coordinates of *A*, *B*, and *C* are then determined in the *xyz* system by

$$x_A = S_{TA}\sin(U_A)\cos(V_A) \quad (11)$$

$$y_A = S_{TA}\cos(U_A)\cos(V_A) \quad (12)$$

$$z_A = S_{TA}\sin(V_A) \quad (13)$$

$$x_B = S_{TB}\sin(U_B)\cos(V_B) \quad (14)$$

$$y_B = S_{TB}\cos(U_B)\cos(V_B) \quad (15)$$

$$z_B = S_{TB}\sin(V_B) \quad (16)$$

$$x_C = S_{TC}\sin(U_C)\cos(V_C) \quad (17)$$

$$y_C = S_{TC}\cos(U_C)\cos(V_C) \quad (18)$$

$$z_C = S_{TC}\sin(V_C) \quad (19)$$

Finally, the coordinates of the hidden point *D* are calculated as follows

$$x_D = x_C + lS_{CD} \quad (20)$$

$$y_D = y_C + mS_{CD} \quad (21)$$
$$z_D = z_C + nS_{CD} \quad (22)$$

where l, m, and n are the direction cosines of the bar which are given by

$$l = (x_C - x_A) / S_{AC} \quad (23)$$

$$m = (y_C - y_A) / S_{AC} \quad (24)$$

$$n = (z_C - z_A) / S_{AC} \quad (25)$$

III. ERROR PROPAGATION

The coordinates of the hidden point D, given by (20)–(22), are implicit functions of the measured horizontal and vertical angles. Therefore, the measurement errors in the angles will affect the standard error in the coordinates through error propagation. The error propagation is quite complex since it will propagate through (1)–(19) to the coordinates of D. Assuming that the measurement errors of the angles are independent, the standard error of the coordinates of D can be written as [7, 8]

$$\sigma^2_{x_D} = \sum_i^6 \left[\frac{\partial x_D}{\partial x_i}\right]^2 \sigma^2_{xi} \quad (26)$$

$$\sigma^2_{y_D} = \sum_i^6 \left[\frac{\partial y_D}{\partial x_i}\right]^2 \sigma^2_{xi} \quad (27)$$

$$\sigma^2_{z_D} = \sum_i^6 \left[\frac{\partial z_D}{\partial x_i}\right]^2 \sigma^2_{xi} \quad (28)$$

where $\partial x_D / \partial x_i$ is the first derivative of x_D with respect to x_i, where i = 1,2, …, 6 and x_i refers to the six horizontal and vertical angles (U_A, U_B, U_C, V_A, V_B, and V_C) and σx_i is the measurement error of x_i. The terms $\partial y_D / \partial x_i$ and $\partial z_D / \partial x_i$ are defined similarly. The error propagation involves 18 first derivatives (six for each of the three coordinates of D) as indicated by (26)–(28). Since the first derivatives are complex, they are obtained using MATLAB [9].

The point standard error of D is then given by

$$\sigma_D = (\sigma^2_{xD} + \sigma^2_{yD} + \sigma^2_{zD})^{0.5} \quad (29)$$

To appreciate the complexity of the first derivatives, the first derivative of x_D with respect to U_A (as an example) is presented in Appendix I.

IV. EVALUATION RESULTS

A. Effect of Changing Location of Fixed Points

This example is an actual application conducted by Antonopoulos [5] to determine the position of a hidden point in the Oil Refinery installations at Aspropyrgos, Athens. The application involved a 4-m scaled invar bar suitably supported by four counter props to avoid differential bending due to bar weight. The horizontal and vertical angles were measured to four points on the bar *A*, *B*, *C*, and *F* at indications 0, 1, 2, and 3 m, respectively, using a total station (Table 1).

TABLE I
OBSERVED ANGLES TO THE BAR FOR EXAMPLE 1 [5]

Point	Angle [a]	
	Bearing (grad)	Vertical (grad)
A	384.9002	13.3908
B	395.5674	8.9314
C	4.6436	4.8622
F	12.1700	1.3790

[a] These angles are listed in *grads* and in this study they were multiplied by (360/400) to convert them into *degrees* (the grad is 1/400 of a full circle).

Since only three observed points are needed for the solution, a least-squares solution was used. The observed angles have a standard error of about ±2". The station was mounted on a chained tripod and centered above a marked point *T'* on the ground floor and the instrument height *h* was 1.5365 m determined by precise levelling. The origins of bearings and vertical angles, the centering of the theodolite, and the scaling of the bar are considered practically errorless. The standard deviation of the coordinates computed by Antonopoulos [5, 10] ranged from 0 to $\pm 5.9 \times 10^{-4}$ m. The positioning results are shown in Table 2.

TABLE II
RESULTS OF THE POINT COORDINATES OF EXAMPLE 1 [5]

Point	Coordinates		
	x(m)	y(m)	z(m)
A	−1.1840	4.8980	1.0758
B	−0.3765	5.3988	0.7643
C	0.4311	5.8995	0.4527
F	1.2386	6.4003	0.1412
D [a]	2.0462	6.9011	−0.1704

[a] Coordinates of D are based on the four fixed-point observations.

To evaluate the effect of the locations of the fixed points, the position accuracy of four combinations (each has three points) of the four points observed by Antonopoulos [5] were examined. Since there are observations to four points on the bar A, B, C, and F that are one meter apart, the combinations tested and the corresponding distances in meters between the points were: ABC (1, 1), ABF (1, 2), ACF (2, 1), and BCF (1, 1). Note that the hidden point is D.

The corresponding horizontal and vertical angles of Table 1 are then used to determine the position accuracy for each combination. The results are shown in Table 3. For this example, the point standard error is the largest for combination BCF and the smallest for combination ABF and ACF. The combination BCF is the worst since its three vertical angles are the smallest and one of its horizontal angles is small. On the other hand, the best combinations correspond to horizontal and vertical angles that are larger in general.

TABLE III
EFFECT OF THE LOCATIONS OF THE BAR FIXED POINTS

Var.[a]	Combinations of Three Observed Points			
	1	2	3	4
	ABC	ABF	ACF	BCF
x_D	2.0464	2.0463	2.0461	2.0459
y_D	6.9010	6.9012	6.9011	6.9005
z_D	-0.1706	-0.1703	-0.1703	-0.1702
σ_{xD}	0.00037	0.00016	0.00019	0.00043
σ_{yD}	0.00027	0.00021	0.00018	0.00081
σ_{zD}	0.00022	0.00010	0.00011	0.00014
σ_D	0.00050	0.00028	0.00028	0.00093

[a] Coordinates of D are based on the corresponding three fixed-point observations.

For example, for combination BCF the horizontal angles (in radians) are 6.2136, 0.0729, and 0.1912 and the vertical angles are 0.1403, 0.0764, and 0.0217. For combination ABF, the horizontal angles are 6.0460, 6.2136, and 0.1912, and the vertical angles are 0.2103, 0.1403, and 0.0217. It is clear that the locations of the fixed points affect the magnitude of the angles and in turn position accuracy. These angles depend on the relative locations of the fixed points with respect to the observation station. In this example, the results suggest that the observation of the lowest three points BCF would not be a good strategy.

B. *Effect of Bar Inclination*

The effect of the inclination angle of the bar on the position accuracy of point D was evaluated using the results of Example 1 (combination ABC) as a starting step to establish the initial geometry of the bar. The bar vertical angle θ was changed by rotating the bar around point D, where the rotation was made in a vertical plane through the initial bar position (Fig. 2). The corresponding simulated horizontal and vertical angles of points A, B, and C are then calculated and the position accuracy is determined.

The vertical angle of bar AD with the horizontal plane, θ_o (Fig. 2) corresponds to combination ABC of Example 1. Using the results of the x and y coordinates of points A and D of this example, the angle θ_o is given by

$$\theta_o = \sin^{-1}[(z_A - z_D)/S_{AD}] \tag{30}$$

Then, the lengths TA', TD', and $A'D'$ and the angles β and φ are calculated. The angle η is then given by

$$\eta = 90^o - \beta - \varphi \tag{31}$$

where η = angle between TD' and the y-axis, β = angle between $A'D'$ and TD' and φ = angle between $A'D'$ and the x-axis. Both angles remain unchanged as the vertical angle of the bar changes.

For any observation point, say C, on an inclined bar with a given angle θ (Fig. 2), the horizontal and vertical angles are then calculated as follows,

$$D'C' = S_{CD}\cos(\theta) \tag{32}$$

$$CC' = S_{CD}\sin(\theta) + z_D \tag{33}$$

$$TC' = [(TD')^2 + (D'C')^2 - 2(TD')(D'C')\cos(\beta)]^{0.5} \tag{34}$$

$$\alpha = \cos^{-1}\{[(TD')^2 + (TC')^2 - (D'C')^2] / [2(TD')(TC')]\} \tag{35}$$

$$U_C = 360^o - \alpha + \eta \tag{36}$$

$$V_C = \tan^{-1}(CC'/TC') \tag{37}$$

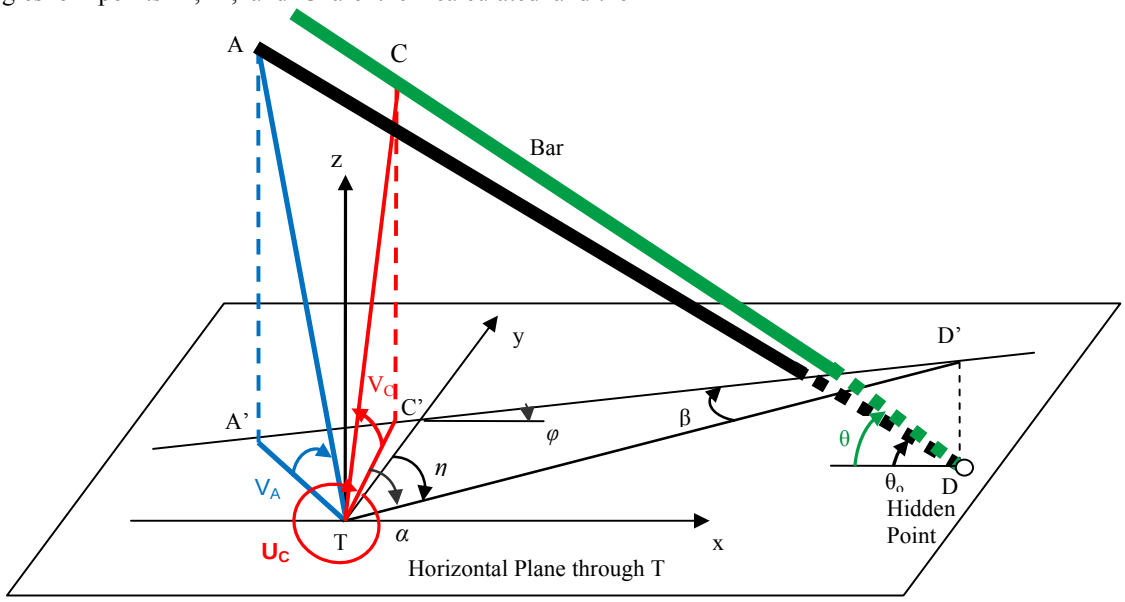

Fig. 2 Geometry of changing the bar vertical angle θ

The horizontal and vertical angles for points A and B are calculated similarly.

To evaluate the position accuracy, the angle θ was changed from 5° to 90° using an increment of 5°. The corresponding standard errors of the coordinates are calculated. Note that in all cases the resulting coordinates of point D were identical to the coordinates of D (Table 1) which is fixed during the simulation of the horizontal and vertical angles of the bar fixed points. This has served as a verification of the developed simulation procedures.

The standard errors are shown in Figs. 3–5. The standard error in x_D decreases as the vertical angle of the bar increases to about 50° and then increases for larger vertical angles of the bar. The standard errors of y_D and z_D increase through the entire range of θ.

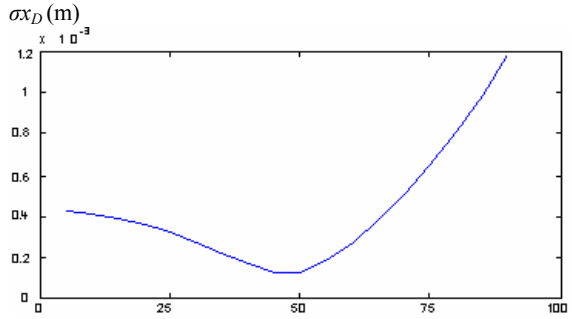

Bar vertical angle, θ (degrees)

Fig. 3 Standard error of the coordinates σx_D

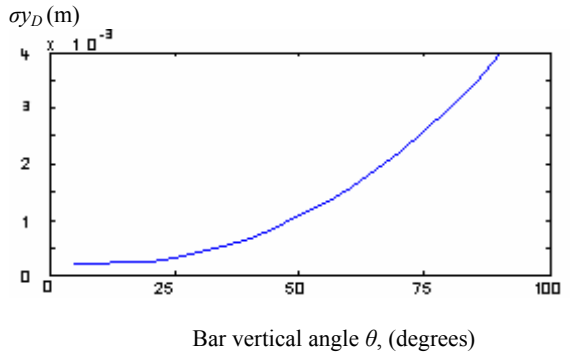

Bar vertical angle θ, (degrees)

Fig. 4 Standard error of the coordinates σy_D

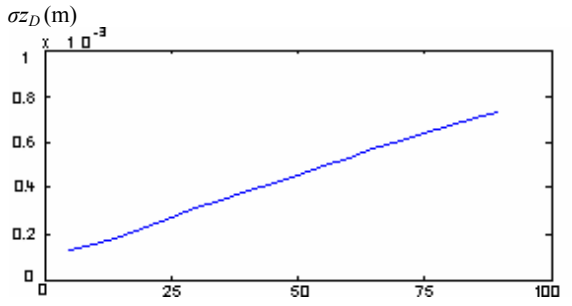

Bar vertical angle θ, (degrees)

Fig. 5 Standard error of the coordinates σz_D

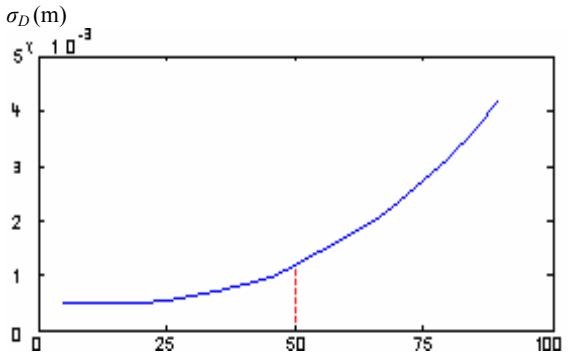

Bar vertical angle, θ (degrees)

Fig. 6 Standard error of the coordinates σ_D (Combination ABC)

The point standard error is shown in Fig. 6. This error remains fairly constant until about θ = 30° and start to moderately increase to about θ = 50°. For larger vertical angles, the standard error substantially increases and becomes about 8 times its value for small bar vertical angles.

Note that the point standard error of Fig. 6 has a minimum point at about θ = 20°, but this point is not clear in the figure. This trend is caused by the nature of the angles that are involved in the calculations of the standard error**.** While the vertical angles increase as the bar vertical angle increases, other angles become small which would have a detrimental effect on error propagation.

C. Effect of Bar Inclination and Combination of Observed Points

Since the values of the horizontal and vertical angles for the observed three points on the bar, it is expected that the position error of the coordinates of D (σ_D), would depend on both the locations of the observed points and the bar vertical angle θ. To evaluate this effect, the relationship between σ_D and θ was established for the worst combination of observed points BCF (see Table 3). A comparison of the standard error of fixed-point combinations is shown in Fig. 7, where combinations 1–4 refer to ABC, ABF, ACF, and BCF, respectively. The 3D representation is used for illustration purposes only, noting that combination 4 (BCF) may be viewed as a simple shift of one meter of combination 1 (ABC). The red arrow approximately refers to the actual bar vertical angle corresponding to Section 3A (θ_o = 18.2°). It is clear from the figure that the standard error of D varies significantly with the change in the bar inclination angle and the locations of the observed points on the bar.

To quantitatively illustrate the effect of the bar vertical angle and fixed-point locations, the distribution of σ_D is shown for the four combinations in Fig. 8. The graph for combination 1 (ABC) is the same as that of Fig. 6, where the bars correspond to bar vertical angle θ ranging from 5° to 90°. The bars for the other two combinations correspond to the same range of θ.

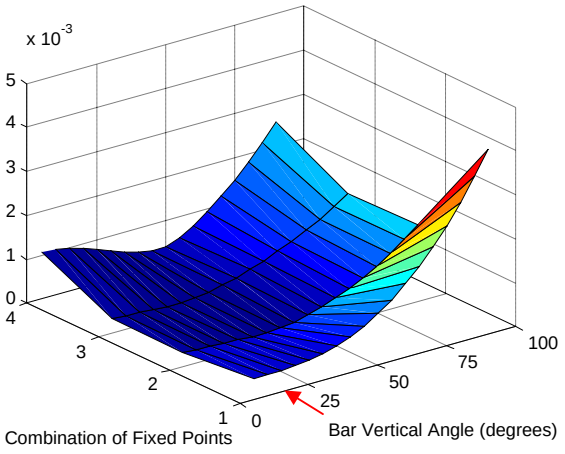

Fig. 7 Standard error σ_D for various fixed-point combinations

As noted, for combination 4 (BCF) σ_D is large for small θ, decreases to a minimum at about 50°, remains almost flat to about 60°, and then sharply increases for larger values of θ. The standard errors for combinations 1 and 4 for θ = 50° are σ_D = 0.0012 m and 0.0004 m, respectively. This interesting trend shows that although combination 1 was better than combination 4 for the actual observations (see Table 3), the minimum σ_D for combination BCF is in fact three times smaller than the corresponding value for combination BCF.

Combinations 2 (ABF) and 3 (ACF) exhibit a similar trend to that of combination 4 except that the minimum value occurs at a vertical angle of about 30°, where σ_D is about 0.00024 m and 0.00026 m, respectively.

It is clear from Fig. 8 that combination 1 is sometimes better and sometimes worse than combination 4, depending on the bar vertical angle. In general, the optimal bar vertical angle depends on the locations of the observed points. In this case study, a bar vertical angle θ = 30°–50° is considered good for all combinations.

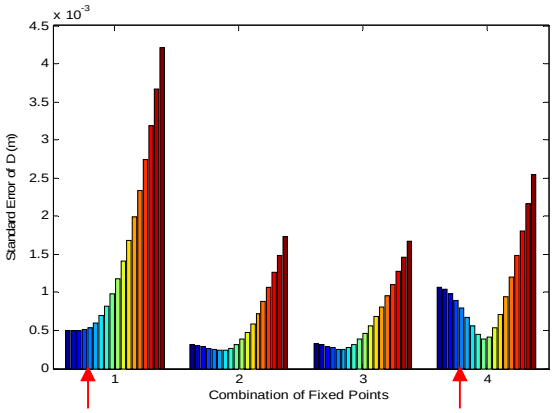

Fig. 8 Comparison of the standard error σ_D for fixed-point combinations ABC(1), ABF(2), ACF(3), and BCF(4)

V. CONCLUSIONS

Error propagation has been conducted in the literature to examine position accuracy in a number of surveying applications [11, 12]. This paper has addressed position accuracy of the hidden-point bar method. The study has investigated the effect of the measurement errors of the vertical and horizontal angles on the overall accuracy of the determined hidden point. The paper focused on the effect of bar geometry on the standard error of the estimated coordinates of the hidden point. Three geometric effects were examined: (a) effect of changing the locations of the fixed (observed) points, (b) effect of the bar inclination angle, and (c) the combined effect of the bar inclination angle and the locations of the fixed points.

The results show that the locations of the fixed points on the bar affect the magnitude of the angles. The results show that the position accuracy depends on the relative position of the fixed points with respect to the observation station. In addition, the study shows a general trend of steady standard error of the estimated hidden-point with the increase in the bar vertical inclination angle until an angle of about 30°–50°. The results indicate that there is an optimal combination of the bar vertical angle and the locations of the fixed points. Perhaps, the best strategy would be to implement an inclination angle in the preceding range and select the fixed points in such a way to avoid very small or very large angles.

Future research may be conducted to evaluate the effects of other geometric elements of the hidden-point bar method, such as the location of the observing station, on the overall accuracy of the determined hidden point.

APPENDIX 1: EXAMPLE OF FIRST DERIVATIVES

To illustrate the complexity of the first derivatives of the coordinates of D, the first derivative of x_D with respect to U_A is shown below.

$$\begin{aligned}\partial x_D / U_A = {} & - S_{BC} \cos(E)\, F \sin(U_C) \cos(V_C) / \{ (1 + [D^2 / \sin^2(C)]) (1 - B^2)^{0.5} \} \\ & + \{ - S_{BC} \cos(E)\, F \sin(U_C) \cos(V_C) / \{ (1 + [D^2 / \sin^2(C)]) (1 - B^2)^{0.5} \} \\ & + S_{AB} \cos(E)\, F \sin(U_A) \cos(V_A) / \{ (1 + [D^2 / \sin^2(C)]) (1 - A^2)^{0.5} \} \\ & + S_{AB} \sin(F) \sin(U_A) \cos(V_A)\ A \cos(V_B) \sin(- U_B + U_A) / (1 - A^2)^{1.5} \\ & - S_{AB} \sin(F) \cos(U_A) \cos(V_A) / (1 - A^2)^{0.5} \} \\ & S_{CD}/(S_{AB} + S_{BC}) \end{aligned} \quad (38)$$

where

$$A = \sin(V_A) \sin(V_B) + \cos(V_A) \cos(V_B) \cos(- U_B + U_A) \quad (39)$$

$$B = \sin(V_B) \sin(V_C) + \cos(V_B) \cos(V_C) \cos(- U_C + U_B) \quad (40)$$

$$C = \cos^{-1}(A) + \cos^{-1}(B) \tag{41}$$

$$D = \{ (1 - A^2)^{0.5} / [S_{AB} (1 - B^2)^{0.5}] \} - \cos(C) \tag{42}$$

$$E = \cos^{-1}(B) + \cot^{-1}[D / \sin(C)] \tag{43}$$

$$\begin{aligned} F = \{ & S_{BC} A \cos(V_A) \cos(V_B) \sin(-U_B + U_A) \\ & / [(1 - A^2)^{0.5} S_{AB} (1 - B^2)^{0.5}] + \sin(C) \cos(V_A) \\ & \cos(V_B) \sin(-U_B + U_A) / (1 - A^2)^{0.5} \} / \sin(C) \\ & - D \cos(C) \cos(V_A) \cos(V_B) \sin(-U_B + U_A) \\ & / [\sin^2(C) (1 - A^2)^{0.5}] \end{aligned} \tag{44}$$

ACKNOWLEDGMENT

Research funding provided by the National Sciences and Engineering Research Council of Canada is gratefully acknowledged. The authors would like to thank Wai Yeung Yan for assistance in producing the graphs used in this study.

REFERENCES

[1] A. L. Allan, *Practical surveying and computations*. Butterworth-Heinemann, Oxford, U.K, 1997.
[2] W. F. Teskey, R. J. Fox, and D. H. Adler, "Hidden point bar method for precise heighting." *J. Survey. Eng.*, vol. 130, no. 4, pp. 179–182, 2004.
[3] L. M. Sebert, "Resections revisited." *Geomatica*, vol. 50, no. 3, pp. 310–311, 1996.
[4] W. F. Teskey, B. Paul, and W. J. Teskey, 2005. "Hidden point bar method for high-precision industrial surveys." *J. Survey. Eng.*, vol. 131, no. 4, pp. 103–106, 2005.
[5] A. Antonopoulos, "Fixation by Hidden Points Bar from One Theodolite." *J. Survey. Eng.*, vol. 131, no. 4, pp. 113–117, 2005.
[6] M. Recoskie, L. Le, and M. Berber, Current technology and new techniques for total station surveys of inaccessible points. *CD-Rom Proceedings, Annual Conference of the Canadian Society for Civil Engineering*, Quebec, QC, 2008.
[7] J. M. Anderson, and E. M. Mikhail, *Surveying: Theory and practice*. McGraw Hill, New York, ch. 2, 1998.
[8] Ghilani, C.D., and P.R. Wolf, *Adjustment computations: Spatial data analysis*. John Wiley & Sons , New York, ch. 6, 2006.
[9] P. Venkataraman, *Applied optimization with MATLAB® programming*. John Wiley, New York, U.S.A., 2002.
[10] A. Antonopoulos, *Personal notes on industrial surveying practicals*. University College London, London, 1994.
[11] S. M. Easa, "Direct distance-based positioning without redundancy – In land surveying." *J. Survey. and Land Info. Science*, vol. 67, no. 2, pp. 69–74, 2007.
[12] E. El-Hasan, "Analysis of the three-point resection accuracy." *The Australian Surveyor*, vol. 34, no. 7, pp. 716–727, 1989.

Said Easa is Professor with the Department of Civil Engineering at Ryerson University, Toronto, Ontario, Canada. He served as Department Chair during 2000–2006. He earned his B.Sc. from Cairo University, M.Eng. from McMaster University (Canada) and Ph.D. from University of California at Berkeley in 1982. His areas of research include highway geometric design, road safety, and human factors. He is Associate Editor of the Journal of Transportation Engineering, American Society of Civil Engineers (ASCE) and author of the "Geometric Design" chapter in the 2002 U.S. Civil Engineering Handbook. He has published extensively in refereed journals and his work has received from ASCE the 2001 Frank M. Masters Transportation Engineering Award for outstanding contributions to the profession and the 2005 Wellington M. Arthur Prize for best journal paper.

Ahmed Shaker is Assistant Professor with the Department of Civil Engineering at Ryerson University, Toronto, Ontario, Canada. He earned his B.Sc. and M.Sc. from Cairo University, and Ph.D. from Hong Kong Polytechnic University, Hong Kong. His research interests cover the fields of satellite sensor modelling, image segmentation and classification, change detection and 3D modelling. He is the recipient of the Marie Curie Incoming International Fellowship, one of the prestigious individual fellowships under the Sixth Framework Program offered by the European Union. He is also the recipient of the National Science Progress Award in Surveying and Mapping from the Chinese National Congress in 2005. He has several publications in international journals and is an active member of several scientific international organizations.